

Effects of substituting rare-earth elements for scandium in a precipitation-strengthened Al–0.08 at. %Sc alloy

Richard A. Karnesky,* Marsha E. van Dalen, David C. Dunand and David N. Seidman

Department of Materials Science and Engineering, 2220 Campus Drive, Northwestern University, Evanston, IL 60208-3108, USA

Received 30 April 2006; accepted 16 May 2006

Available online 19 June 2006

The microhardness of Al–0.06 Sc–0.02 RE alloys (at.%, with RE (rare-earth) = Dy, Er, Gd, Sm, Y, or Yb) is measured as a function of aging time at 300 °C. As compared to Al–0.08 Sc, the ternary alloys exhibit: (i) the same incubation time, except for Al–0.06 Sc–0.02 Yb which hardens much faster; (ii) the same or reduced peak microhardnesses (which are higher than for Al–0.06 Sc); and (iii) the same over-aging behavior. All REs segregate to the core of $\text{Al}_3(\text{Sc}_{1-x}\text{RE}_x)$ precipitates.

© 2006 Acta Materialia Inc. Published by Elsevier Ltd. All rights reserved.

Keywords: Aluminum alloys; Scandium; Rare-earth elements; Lanthanides; Precipitation strengthening

Al–Sc alloys are strong at ambient and elevated temperatures due to the presence of elastically-hard, coherent, nanosized Al_3Sc (L_{12}) precipitates, which exhibit a high number density, a low coarsening rate, and excellent stability at elevated temperatures [1–4]. Ternary additions to Al–Sc alloys of Mg [5], Ti [6], or Zr [7] decrease cost and improve mechanical properties by solid-solution strengthening (as for Mg) or by substituting for Sc in Al_3Sc precipitates (as for Ti and Zr [8–11]). Ti and Zr diffuse significantly more slowly than Sc in Al [12–14] and decrease the lattice parameter mismatch between the α -Al matrix and the precipitates [15]. While both of these attributes increase coarsening resistance, the latter may decrease creep resistance by reducing elastic interactions with dislocations during climb bypass [6,7,16]. The ideal ternary additions for creep-resistant Al–Sc alloys should thus exhibit high solubility in Al_3Sc and low diffusivity in α -Al (like Ti and Zr), while moderately increasing the lattice parameter of Al_3Sc (unlike Ti and Zr) [17]. These three attributes are displayed by many rare-earth elements (RE), including Y, Sm, Gd and the lanthanides heavier than Gd [15,18–26]. Their diffusivity in α -Al is unknown, but is anticipated to be similar to that of light REs, which diffuse more slowly than Sc [14,27]. Additionally, these REs are less expensive than Sc [28].

Sawtell and Morris [23,24] found that additions of 0.3 at.% Er, Gd, Ho, or Y improve the ambient-temperature tensile strength of Al–0.3 at. %Sc alloys by ca. 11–23%. They attributed this result to elastic effects associated with the larger radii of RE atoms with respect to Sc. Very small precipitates were observed by TEM after aging, which were assumed to be $\text{Al}_3(\text{Sc}_{1-x}\text{RE}_x)$. Because the RE and Sc exceeded their solid solubilities in aluminum, these rapidly-cooled alloys were not homogenized; given the high partitioning ratio of Al–RE alloys [17], segregation may have led to an inhomogeneous distribution of precipitates.

In the present study, we investigated dilute Al–0.06 at. %Sc alloys with small additions of 0.02 at.% RE, thereby permitting homogenization. We measured their microhardness after precipitation heat-treatments at 300 °C and also used a local-electrode atom-probe (LEAP) tomograph (Imago Scientific Instruments (Madison, WI)) to study their chemical composition at the atomic level.

Six Al–0.06 at.% Sc–0.02 at.% RE (denoted by Al–Sc–RE) alloys were studied for the following REs: Y, Sm, Gd, Dy, Er, or Yb. The four other Al_3Sc -soluble lanthanides (Tb, Ho, Tm, and Lu) were not considered due to their higher cost. The relatively low RE concentration was chosen to increase the probability for the alloy to remain in the single-phase α -Al field during homogenization, as the exact solid-solubility of these REs in α -Al is very small and unknown quantitatively.

The alloys were dilution-cast in a zirconia-coated alumina crucible in a resistively-heated furnace at 750 °C in

* Corresponding author. Tel.: +1 847 491 3575; fax: +1 847 467 2269; e-mail: karnesky@northwestern.edu

Table 1. Composition of Al–0.06 Sc–0.02 RE (at.%) alloys as measured by direct coupled plasma (DCP) spectroscopy and by LEAP spectrometry^a

Alloy	Sc Content from DCP (at.%)	RE Content from DCP (at.%)	Sc Content from LEAP (at.%)	RE Content from LEAP (at.%)
Al–Sc	0.060(3)	–	0.0571(4)	–
	0.082(3)	–	0.0865(6)	–
Al–Sc–Y	0.061(3)	0.0188(15)	0.0622(13)	0.0191(11)
Al–Sc–Sm	0.059(3)	0.0250(9) ^b	0.0561(4)	0.0042(9) ^b
Al–Sc–Gd	0.061(3)	0.0182(9)	0.0653(11)	0.0150(3)
Al–Sc–Dy	0.058(3)	0.0236(8)	0.0618(9)	0.0208(9)
Al–Sc–Er	0.064(3)	0.0220(8)	0.0695(5)	0.0220(10)
Al–Sc–Yb	0.058(3)	0.0242(8)	0.0593(10)	0.0340(8)

^a Uncertainty is given in parentheses after the least significant digits to which it applies.

^b Al–Sm precipitates present after homogenization are measured by DCP, but not by LEAP spectrometry, thus explaining the discrepancy between measurements.

air, using 99.99 Al (all compositions hereafter are given in at.%), an Al–1.2 Sc master alloy (Ashurst Technology Ltd., Baltimore, MD, and KB Alloys, Inc., Reading, PA), and Al–1 RE master alloys. These master alloys were produced by non-consumable electrode arc-melting from 99.99 Al and 99.9 RE, the latter supplied by Stanford Materials (Aliso Viejo, CA). After thoroughly stirring, the melt was cast into a graphite mold resting on a large copper platen to insure relatively rapid solidification and cooling. Chemical compositions of arc-melted master alloys and as-homogenized dilute alloys were determined by direct-current plasma emission spectroscopy by ATI Wah Chang (Albany, OR) and by LEAP spectrometry, as reported in Table 1.

The cast alloys were homogenized in air at 640 °C for 72 h and then water-quenched. Aging was performed at 300 °C for various times and was terminated by a water quench. Aging for times of 5 min. (0.08 h) or longer was performed in air, while the shorter aging treatments for Al–Sc–Yb were performed in molten salt. Vickers microhardness was measured using a 200 g weight at ambient temperature on samples ground to a 1 μm surface finish.

LEAP tomographic sample blanks were produced by mechanically grinding material to a square cross-section of ca. 200 × 200 μm². An initial electropolishing with a solution of 10 vol.% perchloric acid in acetic acid was

followed by a final polishing with a solution of 2 vol.% perchloric acid in butoxyethanol. Three-dimensional tomographic reconstructions were obtained, using Imago's computer program IVAS and proximity histograms (proxigrams) [29] were calculated employing IVAS and Apex software [30], utilizing an isoconcentration surface of 5 at.% Sc. The average precipitate and matrix concentrations were calculated by employing the fraction of total atoms in the pertinent volume.

Figure 1(a) and (b) display the microhardness as a function of aging time at 300 °C for all alloys studied. As compared to an Al–0.08 Sc, it is clear that partial replacement of Sc by RE does not affect the incubation periods of ca. 15 min (which is decreased from ca. 3 h for Al–0.06 Sc [31,32]), except for Al–Sc–Yb for which there is no measured incubation period.

The Al–Sc–Gd and Al–Sc–Sm peak microhardnesses, while appreciably higher than that of binary Al–0.06 Sc, are also significantly lower than for the other four Al–Sc–RE alloys and Al–0.08 Sc (Table 1). Some of this difference may be attributable to the lower solubility of Gd and Sm in Al₃Sc [19–21], resulting in a lower volume fraction of precipitates (0.28 ± 0.01% for Al–Sc–Gd compared with 0.31 ± 0.01% for Al–Sc–Er, as estimated from the LEAP tomographic concentrations). Furthermore, micron-sized Al–Sm precipitates were observed at grain boundaries of homogenized Al–Sc–Sm. This

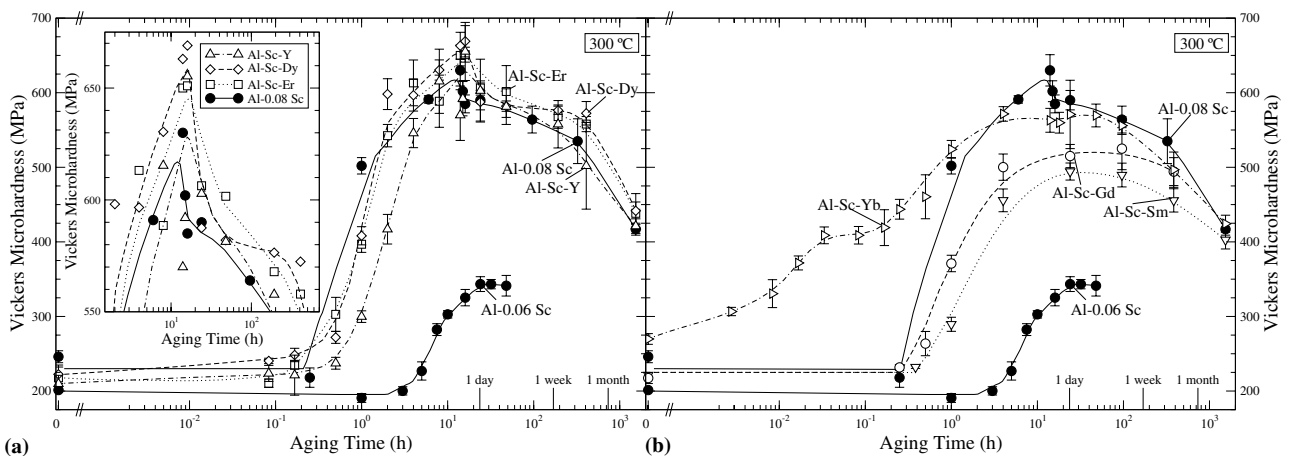


Figure 1. (a) and (b) Vickers microhardness vs. aging time at 300 °C for Al–0.06 Sc–0.02 RE, Al–0.06 Sc, and Al–0.06 Sc [31,32]. Error bars are 1 standard deviation from the mean.

placed an additional limit on the maximum obtainable volume fraction of $\text{Al}_3(\text{Sc}_{1-x}\text{Sm}_x)$ precipitated during aging.

Within one standard deviation, Al–Sc–Y, Al–Sc–Dy, and Al–Sc–Er have the same peak microhardness as Al–0.08 Sc. The mean measured microhardnesses in the peak regions of these three alloys are, however, all higher than the peak microhardness of Al–0.08 Sc. Minor volume fraction differences based on differing solute contents (Table 1) are not sufficient to explain this effect, whose causes may instead be a higher resistance to: (a) shearing of small precipitates; and/or (b) bypass of large precipitates (the transition between shearing and bypassing occurring at radii of ca. 2 nm in prior studies of Al–Sc alloys [5,7,23,31,32]). The shearing stress scales with the $3/2$ power of the constrained lattice parameter mismatch [33] due to coherency strengthening, and the three $\text{Al}_3(\text{Sc}, \text{RE})$ phases have a greater lattice parameter mismatch with Al than Al_3Sc [15,18–26,34]. The Orowan strengthening scales with $\ln(R)/R$, where R is the precipitate radius [33], so the higher strengths could be the result of smaller precipitates, assuming the same volume fraction of precipitates.

Figure 2 displays LEAP tomographic reconstructions for Al–Sc–Er and Al–Sc–Gd aged at 300 °C for 24 h. The Al–Sc–Er alloy has the larger number density ($(1.1 \pm 0.1) \times 10^{23} \text{ m}^{-3}$, compared with $(3.8 \pm 0.3) \times 10^{22} \text{ m}^{-3}$ for Al–Sc–Gd) of smaller precipitates ($\langle R \rangle = 1.9 \pm 0.3 \text{ nm}$, compared with $2.4 \pm 0.3 \text{ nm}$ for Al–Sc–Gd). Assuming Orowan strengthening, this trend in precipitate mean radius is in agreement with the trend in peak microhardness for these alloys: the measured precipitate mean radii and volume fractions predict an Orowan stress of $169 \pm 29 \text{ MPa}$ for Al–Sc–Er and $139 \pm 19 \text{ MPa}$ for Al–Sc–Gd (using equations reported in Ref. [6,7,31–33]).

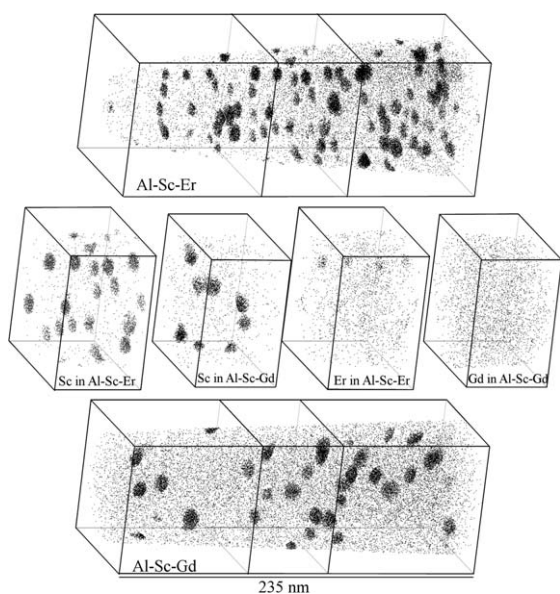


Figure 2. LEAP tomographic reconstructions of Al–0.06 Sc–0.02 Er and Al–0.06 Sc–0.02 Gd (at.%) aged for 24 h at 300 °C. Al–Sc–Er shows a larger number density of smaller precipitates than Al–Sc–Gd. Er segregates more to $\text{Al}_3(\text{Sc}_{1-x}\text{RE}_x)$ precipitates than does Gd.

A proxigram showing the concentration of Sc and RE (RE = Er, Gd) as a function of radial distance from the α -Al/precipitate interface is presented in Figure 3. It is apparent that both RE elements segregate to the cores of the precipitates, unlike Ti [6] and Zr [8–11] that segregate to the surface of the precipitates. Thus, in all cases, the elements increasing the α -Al/precipitate misfit segregate to the precipitate core, leading to a monotonic gradient of lattice misfit from the core to the surface of the precipitates, which may be expected to minimize the elastic misfit energy. A much larger fraction of Sc atoms is replaced by Er than by Gd in the precipitates: 17.42 ± 0.04 vs. 8.22 ± 0.03 at.%, as calculated by averaging the concentration over the precipitate volume. This may reflect the higher solubility of Er in Al_3Sc (100% vs. 15% maximum replacement for Gd), and contributes to the higher peak hardness, since the volume fraction of precipitates in the Al–Sc–Er alloy is greater than in the Al–Sc–Gd alloy.

The much smaller incubation time for Al–Sc–Yb as compared to all other alloys is indicative of a significantly larger diffusivity for Yb in Al as compared to Sc and the other RE elements studied. This hypothesis is supported by the LEAP tomographic study of Al–Sc–Yb alloy aged for 5 min at 300 °C, which showed Yb-rich precipitates with minor Sc content. For a longer aging time of 6 h, Al–Sc–Yb exhibits $\text{Al}_3(\text{Sc}_{1-x}\text{Yb}_x)$ precipitates with Yb as a minor element, similar to Al–Sc–Er and Al–Sc–Gd (Fig. 3). This anomalous diffusion/precipitation behavior may be linked to Yb having the lowest melting point and largest metallic radius of the six REs studied here.

In summary, a study of the precipitation hardening of Al–0.06 Sc–0.02 RE (in at.%, with RE = Dy, Er, Gd, Sm, Y, or Yb) aged at 300 °C was performed. As compared to Al–0.08 Sc, incubation time, peak hardness, and over-aging behavior were mostly unaffected by the partial replacement of Sc by RE. The exceptions included Sm (which formed primary precipitates and

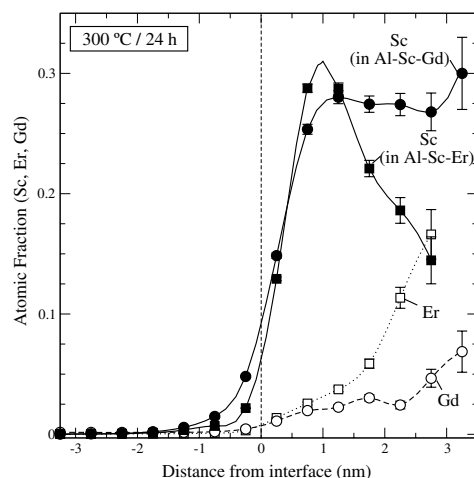


Figure 3. Proximity histogram for the LEAP tomographic reconstructions displayed in Fig. 3 showing the average concentration of Sc, Er, or Gd as a function of distance from the α -Al/ $\text{Al}_3(\text{Sc}_{1-x}\text{RE}_x)$ heterophase interface, as defined by a 5 at.% Sc isoconcentration surface. Concentration error bars are calculated as $\sigma_c = \sqrt{c(1-c)/N}$, where N is the total number of atoms detected.

dissolved only partially in Al_3Sc , and thus reduced microhardness), Gd (which also dissolved only partially in Al_3Sc , and reduced microhardness), and Yb (which had a much shorter incubation time). LEAP tomographic studies demonstrated that Er and Gd (and therefore probably also the other REs) partitioned to the $\text{Al}_3(\text{Sc}_{1-x}\text{RE}_x)$ precipitates and segregated at their cores.

This research is supported by the US Department of Energy through grant DE-FG02-98ER45721. The LEAP tomograph was purchased with funding from the NSF-MRI (Grant DMR-0420532) and ONR-DUR-IP (Grant N00014-0400798) programs. We thank Ashurst Technology Ltd. and the Los Alamos Neutron Scattering Center (LANSCE) for supplying Al–Sc master alloys. We also thank Mr. Keith Knipling and Prof. Dieter Isheim (Northwestern University) for helpful discussions.

- [1] J. Royset, N. Ryum, *Int. Mater. Rev.* 50 (2005) 19–44.
- [2] E.A. Marquis, D.N. Seidman, *Acta Mater.* 49 (2001) 1909–1919.
- [3] S. Iwamura, Y. Miura, *Acta Mater.* 52 (2004) 591–600.
- [4] L.S. Toropova, *Advanced Aluminum Alloys Containing Scandium: Structure and Properties*, Taylor&Francis, Amsterdam, 1998.
- [5] E.A. Marquis, D.N. Seidman, D.C. Dunand, *Acta Mater.* 51 (2003) 4751–4760.
- [6] M.E. van Dalen, D.C. Dunand, D.N. Seidman, *Acta Mater.* 53 (2005) 4225–4235.
- [7] C.B. Fuller, D.N. Seidman, D.C. Dunand, *Acta Mater.* 51 (2003) 4803–4814.
- [8] B. Forbord, W. Lefebvre, F. Danoix, H. Hallem, K. Marthinsen, *Scripta Mater.* 51 (2004) 333–337.
- [9] C.B. Fuller, J.L. Murray, D.N. Seidman, *Acta Mater.* 53 (2005) 5401–5413.
- [10] A. Tolley, V. Radmilovic, U. Dahmen, *Scripta Mater.* 52 (2005) 621–625.
- [11] E. Clouet, Ph.D. Thesis, Ecole Centrale Paris, 2004.
- [12] T. Marumo, S.I. Fujikawa, K. Hirano, *J. Jpn. Inst. Light Met.* 23 (1989) 17–25.
- [13] D. Bergner, N. van Chi, *Wissenschaftliche Zeitschrift der Padagogischen Hochschule Halle* 15 (1977) 15.
- [14] S.I. Fujikawa, *Defect Diffus. Forum* 143 (1997) 115–120.
- [15] Y. Harada, D.C. Dunand, *Mater. Sci. Eng. A* 329 (2002) 686–695.
- [16] E.A. Marquis, D.C. Dunand, *Scripta Mater.* 47 (2002) 503–508.
- [17] K.E. Knipling, D.C. Dunand, D.N. Seidman, *Z. Metallkd.* 97 (2006) 246–265.
- [18] T.J. Watson. *High Strength Aluminum Alloy*. Patent 6248453, 2001.
- [19] O.I. Zalutskaya, V.G. Kontsevi, M.I. Karamish, V.R. Ryabov, I.I. Zalutsky, *Dopov Akad Nauk A* (1970) 751–753.
- [20] O.I. Zalutskaya, V.R. Ryabov, I.I. Zalutsky, *Dopov Akad Nauk A* (1969) 255–259.
- [21] A. Palenzona, *J. Less-Common Met.* 29 (1972) 289–292.
- [22] G. Petzow, G. Effenberg, *Ternary Alloys: A Comprehensive Compendium of Evaluated Constitutional Data and Phase Diagrams*, VCH, Weinheim, 1988.
- [23] R.R. Sawtell, Ph.D. Thesis, University of California, Berkeley, 1988.
- [24] R.R. Sawtell, J.J.W. Morris, *Exploratory Alloy Development in the System Al–Sc–X*, in: Y.-W. Kim, W.M. Griffith (Eds.), *Dispersion Strengthened Aluminum Alloys*, TMS, Warrendale, PA, 1988, pp. 409–420.
- [25] D.J. Chakrabarti, J.T. Staley, S.F. Baumann, R.R. Sawtell, P.E. Bretz, C.L. Jensen. *Superplastic Aluminum Products and Alloys*. US Patent 5055257, 1991.
- [26] R.R. Sawtell, P.E. Bretz, C.L. Jensen. *Superplastic Aluminum Alloys Containing Scandium*. US Patent 4689090, 1987.
- [27] L.F. Mondolfo, *Aluminum Alloys: Structure and Properties*, Butterworth, London, 1976.
- [28] U.S.G. Survey. *Metal Prices in the United States through 1998*. Reston, VA: US Geological Survey.
- [29] O.C. Hellman, J.A. Vandenbroucke, J. Rüsing, D. Isheim, D.N. Seidman, *Microsc. Microanal.* 6 (2000) 437–444.
- [30] O.C. Hellman, J. Vandenbroucke, J.B. du Rivage, D.N. Seidman, *Mater. Sci. Eng. A* 327 (2002) 29–33.
- [31] E.A. Marquis, D.N. Seidman, D.C. Dunand, *Acta Mater.* 51 (2003) 285–287.
- [32] D.N. Seidman, E.A. Marquis, D.C. Dunand, *Acta Mater.* 50 (2002) 4021–4035.
- [33] E. Nembach, *Particle Strengthening of Metals and Alloys*, Wiley, New York, NY, 1997.